

A Major Combustion Aerosol Event Had a Negligible Impact on the Atmospheric Ice-Nucleating Particle Population

Key Points:

- Ice-nucleating particle concentrations were unaffected by high aerosol loading during Bonfire Night celebrations
- Aerosol concentrations rose by up to a factor of 10 and black carbon by up to a factor of 100 during these bonfire and firework events
- Our limiting active site density for Bonfire Night black carbon is consistent with other recent work with low ice-nucleating activities

Supporting Information:

- Supporting Information S1

Correspondence to:

M. P. Adams,
m.p.adams@leeds.ac.uk

Citation:

Adams, M. P., Tarn, M. D., Sanchez-Marroquin, A., Porter, G. C. E., O'Sullivan, D., Harrison, A. D., et al. (2020). A major combustion aerosol event had a negligible impact on the atmospheric ice-nucleating particle population. *Journal of Geophysical Research: Atmospheres*, 125, e2020JD032938. <https://doi.org/10.1029/2020JD032938>

Received 23 APR 2020

Accepted 21 SEP 2020

Accepted article online 5 NOV 2020

Author Contributions:

Conceptualization: M. P. Adams, M. D. Tarn, D. O'Sullivan, M. A. Holden, B. J. Murray

Data curation: M. P. Adams, G. C. E. Porter, B. J. Murray

Formal analysis: M. P. Adams, M. D. Tarn, D. O'Sullivan, A. D. Harrison, Z. Cui, J. Vergara-Temprado, J. B. McQuaid, B. J. Murray

Funding acquisition: B. J. Murray

Investigation: M. D. Tarn, G. C. E. Porter, D. O'Sullivan, A. D. Harrison, F. Carotenuto, S. N. F. Sikora, J. B. McQuaid, B. J. Murray

Methodology: M. P. Adams, M. D. Tarn, G. C. E. Porter, D. O'Sullivan, A. D. Harrison, F. Carotenuto, M. A. Holden, T. F. Whale, S. N. F. Sikora, I.

(continued)

M. P. Adams¹ , M. D. Tarn^{1,2} , A. Sanchez-Marroquin¹ , G. C. E. Porter^{1,2} , D. O'Sullivan^{1,3} , A. D. Harrison¹ , Z. Cui¹ , J. Vergara-Temprado^{1,4} , F. Carotenuto^{5,6,7} , M. A. Holden^{1,2,8,9} , M. I. Daily¹ , T. F. Whale^{1,8,10} , S. N. F. Sikora¹ , I. T. Burke¹¹ , J.-U. Shim² , J. B. McQuaid¹ , and B. J. Murray¹ 

¹Institute of Climate and Atmospheric Science, School of Earth and Environment, University of Leeds, Leeds, UK, ²School of Physics and Astronomy, University of Leeds, Leeds, UK, ³Now at The Stars Group, Wellington Place, Leeds, UK, ⁴Now at Institute for Atmospheric and Climate Science, ETH Zürich, Zurich, Switzerland, ⁵Institute of Ecology, University of Innsbruck, Innsbruck, Austria, ⁶CNR Institute of BioMeteorology, Florence, Italy, ⁷Now at CNR Institute of BioEconomy, Florence, Italy, ⁸School of Chemistry, University of Leeds, Leeds, UK, ⁹Now at School of Physical Sciences and Computing, University of Central Lancashire, Preston, UK, ¹⁰Now at Department of Chemistry, University of Warwick, Coventry, UK, ¹¹Earth Science Institute, School of Earth and Environment, University of Leeds, Leeds, UK

Abstract Clouds containing supercooled water are important for both climate and weather, but our knowledge of which aerosol particle types nucleate ice in these clouds is far from complete. Combustion aerosols have strong anthropogenic sources, and if these aerosol types were to nucleate ice in clouds, they might exert a climate forcing. Here, we quantified the atmospheric ice-nucleating particle (INP) concentrations during the United Kingdom's annual Bonfire Night celebrations, which are characterized by large amounts of combustion aerosol from bonfires and fireworks. We used three immersion mode techniques covering more than 6 orders of magnitude in INP concentration over the temperature range from -10°C to homogeneous freezing. We found no observable systematic change in the INP concentration on three separate nights, despite more than a factor of 10 increase in aerosol number concentrations, up to a factor of 10 increase in PM_{10} concentration, and more than a factor of 100 increase in black carbon (BC) mass concentration relative to pre-event levels. This implies that BC and other combustion aerosol such as ash did not compete with the INPs present in the background air. Furthermore, the upper limit of the ice-active site surface density, $n_s(T)$, of BC generated in these events was shown to be consistent with several other recent laboratory studies, showing a very low ice-nucleating activity of BC. We conclude that combustion aerosol particles similar to those emitted on Bonfire Night are at most of secondary importance for the INP population relevant for mixed-phase clouds in typical midlatitude terrestrial locations.

Plain Language Summary Liquid water droplets found in clouds can cool to well below 0°C while remaining in the liquid phase (this is known as supercooling). These supercooled droplets can remain liquid down to below around -33°C without freezing, unless there is a certain type of aerosol particle present: an ice-nucleating particle (INP). Hence, INPs have the potential to drastically change the properties and lifetime of clouds, but the sources of INP in the atmosphere are poorly defined. In this study we measured the INP concentration before, during, and after a major combustion aerosol event in the United Kingdom, Bonfire Night. This celebration is characterized by bonfires (primarily made of waste wood, but also containing garden and household waste) and fireworks. We found that aerosol particles emitted during the celebration are not as effective at nucleating ice as aerosol particle already present in the atmosphere. We conclude that aerosol particles emitted from combustion processes such as those observed on Bonfire Night are not an important source of INPs.

1. Introduction

The formation of ice in supercooled water droplets plays a central role in regulating cloud properties, such as radiative forcing and lifetime, as well as the generation of precipitation (Hoose & Möhler, 2012; Kanji et al., 2017; Lohmann et al., 2006; Murray et al., 2012; Rosenfeld et al., 2011). While ice nucleation only

T. Burke, J.-U. Shim, J. B. McQuaid, B. J. Murray

Project administration: M. P. Adams, B. J. Murray

Resources: J. B. McQuaid, B. J. Murray

Software: Z. Cui, J. Vergara-Temprado, I. T. Burke, J. B. McQuaid

Supervision: M. D. Tarn, D.

O'Sullivan, M. A. Holden, I. T. Burke,

J.-U. Shim, J. B. McQuaid, B. J. Murray

Validation: B. J. Murray

Visualization: M. P. Adams, B. J. Murray

Writing - original draft: M. P. Adams, M. D. Tarn, G. C. E. Porter, D.

O'Sullivan, A. D. Harrison, Z. Cui, J.

Vergara-Temprado, M. A. Holden, T. F.

Whale, J. B. McQuaid, B. J. Murray

Writing - review & editing: M. P.

Adams, M. D. Tarn, G. C. E. Porter, D.

O'Sullivan, A. D. Harrison, Z. Cui, J.

Vergara-Temprado, M. A. Holden, T. F.

Whale, J. B. McQuaid, B. J. Murray

occurs spontaneously in supercooled clouds at temperatures below around -33°C (Herbert et al., 2015), ice-nucleating particles (INPs) can catalyze the freezing process at higher temperatures. Clouds composed of supercooled water or mixtures of supercooled water and ice, which are referred to as mixed-phase clouds, exist in the lower to middle troposphere and are susceptible to the presence of INPs. The formation of ice in shallow clouds tends to reduce the amount of liquid water in them and decrease their albedo (Vergara-Temprado et al., 2018). Representing the contribution and evolution of cloud ice processes in both the present day and a future warmer climate is important for obtaining accurate climate predictions (Storelvmo, 2017; Tan et al., 2016). Hence, it is essential that we identify and quantify all relevant sources of INPs to understand their impact on mixed-phase clouds.

In general, it is thought that, in the mixed-phase regime ($\sim -38^{\circ}\text{C}$ to 0°C), ice formation only becomes significant once a liquid cloud exists; hence, the pathways involving liquid water are thought to be most relevant (Ansmann et al., 2009; de Boer et al., 2011; Murray et al., 2012; Westbrook & Illingworth, 2011). INPs are also important for upper tropospheric ice clouds (Cziczo et al., 2013; DeMott, Sassen, et al., 2003), but the pathways of ice formation are distinct under those colder conditions, and we do not consider INPs relevant for in situ formed cirrus type clouds here (Vali et al., 2015). What makes certain aerosol particles effective at nucleating ice under mixed-phase conditions is complex and poorly understood. Recent work indicates that ice-active sites on mineral nucleators require a specific combination of chemistry and topography (Holden et al., 2019), whereas some biological materials, like specific bacteria, have evolved the capacity to produce proteins that nucleate ice (Šantl-Temkiv et al., 2015). As a result of both our limited understanding and also the fact that different materials nucleate ice through different mechanisms, we have no a priori means of establishing if a particular material is an effective ice nucleator. There has been much discussion over whether aerosol from combustion processes is important as INPs, with mixed conclusions (Ardon-Dryer & Levin, 2014; Chen et al., 2018; DeMott, 1990; Grawe et al., 2018; Kanji et al., 2020; Mahrt et al., 2018; McCluskey et al., 2014; Schill et al., 2016; Umo et al., 2015; Vergara-Temprado et al., 2018). This is significant because carbonaceous combustion aerosol, and presumably other aerosol associated with combustion such as ash, has increased in concentration dramatically since pre-industrial times and therefore has the potential to exert a significant anthropogenic impact on clouds and climate (Bond et al., 2013; Lavanchy et al., 1999; Spracklen et al., 2011).

The composition of combustion aerosol is massively variable, depending on fuel types and combustion conditions (Elsasser et al., 2013; Lighty et al., 2000). Soot particles, with characteristic fractal morphologies, are synonymous with incomplete combustion. Once emitted, soot aerosol then evolves through the uptake of other chemical species, undergoing heterogeneous reactions and aggregating with other aerosol types; it is then referred to with the more general term, black carbon (BC) (Petzold et al., 2013). Lower temperature combustion can result in the formation of organic-rich particles, termed tar balls (Adachi & Buseck, 2011; Pósfai et al., 2004). In addition, inorganic components of the fuels can form ash particles that can also be lofted into the atmosphere (DeMott, Cziczo, et al., 2003; Kumai, 1961). Clearly, laboratory studies of ice nucleation by combustion products are valuable, but real-world combustion aerosol is likely to have much more varied compositions and therefore could conceivably have very different ice-nucleating properties.

Previous studies in the field have been carried out to investigate the relationship between combustion and INP concentrations relevant for mixed-phase clouds, with conflicting results. During a field campaign, Twohy et al. (2010) observed that, in mixed-phase clouds, there was a strong correlation between BC and ice crystal concentration, implying that aerosol containing BC may act as INPs. However, ice crystal residues from the same campaign were not obviously enhanced in BC or other combustion aerosol (Pratt et al., 2009). McCluskey et al. (2014) found that a substantial number of INPs (up to 64% for some of the samples) from wildfires and prescribed burns were identified as BC particles via analysis with a scanning electron microscope, while Petters et al. (2009) conducted laboratory burns with controlled fuel types and found that some fuels created aerosols that nucleated ice while others did not. Others have measured INPs emitted from forest fires and shown that aerosol particles produced from biomass burning can act as a source of INPs (Hobbs & Locatelli, 1969; Prenni et al., 2012). For example, Prenni et al. (2012) suggested that while the fraction of aerosol able to nucleate ice is relatively small, the high concentration of particles emitted from a forest fire means that this aerosol could be an important source of INPs. Levin et al. (2016) investigated contributions of BC from biomass burning to the atmospheric INP burden, finding a positive relationship between BC and INP concentrations. Furthermore, observations of ice crystal residues sampled at mountain top

sites revealed that there are instances in which they were composed of BC (Cozic et al., 2008), while in other cases BC was not observed (Baustian et al., 2012; Kamphus et al., 2010).

In addition to the above studies on the activity of wildfires or controlled burns of natural fuels, there have also been studies of aerosol produced by bonfire burning and more general human-related pollution aerosol in which combustion aerosol plays a major role. Ardon-Dryer and Levin (2014) investigated the effect of the Lag BaOmer festival, when bonfires are lit across Israel, on local INP concentrations. They found INP concentrations to be higher before the festival began, despite a clear rise in total aerosol concentration after the start of the festival. Chen et al. (2018) took measurements in Beijing, China, where combustion aerosol is in abundance, over a 30-day field campaign. In this study, no relationship was found between INP concentrations and either total particle number or BC concentration. More recently in Beijing, Bi et al. (2019) also observed no clear relation between INP concentrations and pollution events (defined by the increase in fine mode aerosol along with back trajectories that passed over heavily industrialized areas). A study investigating the potential of a steel mill as a source of INPs found that air influenced by emissions from the steel mill did have higher INP concentrations than ambient air at temperatures above -12°C but concluded that the mill was unlikely to have any effect on the synoptic scale as the INPs were not detectable at distances greater than 15 km (Schnell et al., 1980). Hartmann et al. (2019) measured historic INP concentrations in the European Arctic using ice cores from up to 500 years ago. They found no correlation between increasing anthropogenic aerosol (with BC being specifically measured) reaching the Arctic and INP concentrations, which were found to be similar to present day concentrations and without a long-term trend (i.e., INP concentrations did not increase with increasing anthropogenic emissions). A study combining observational data with model simulations in an effort to understand the potential importance of anthropogenic aerosols as INPs indicated that polluted continental aerosols contain a significant fraction of INPs (Zhao et al., 2019). Whether these INPs were associated with combustion aerosol or other terrestrial INP types is unclear. Overall, the evidence from observations and field campaigns is mixed, without a clear resolution as to whether combustion aerosol is an important source of INPs.

There have also been a number of laboratory studies carried out to investigate the ice-nucleating potential of BC and other combustion aerosol types produced in a variety of ways, again with contrasting results. There is evidence that BC nucleates ice when immersed in (or at least in the presence of) supercooled droplets (DeMott, 1990; Diehl & Mitra, 1998; Fornea et al., 2009; Gorbunov et al., 2001; Kireeva et al., 2009; Popovicheva et al., 2008; Wright et al., 2013). In addition, carbon-based materials including graphene oxides and carbon nanotubes nucleate ice, which shows that carbon-rich materials have the potential to nucleate ice (Alstadt et al., 2017; Bai et al., 2019; Whale, Rosillo-Lopez, et al., 2015). Murray et al. (2012) parameterized data from DeMott (1990), who used soot from an oxygen-deficient acetylene burner, and Diehl and Mitra (1998), who used a kerosene burner, by calculating the ice-active site surface density, $n_s(T)$, of BC, and concluded that BC may be a very important INP type globally. However, more recent work strongly contradicts this conclusion. Schill et al. (2016) found that the concentration of immersion mode INPs produced by an off-road diesel engine was below their limit of detection at -30°C , thus reporting upper limits for the ice-nucleating activity of BC, and suggested that previous literature parameterizations were likely overestimating the importance of BC-based INPs, especially in the Northern Hemisphere. Similarly, measurements reported by Ullrich et al. (2017) showed that droplets containing BC particles in the Aerosol Interaction and Dynamics in the Atmosphere (AIDA) cloud simulation chamber did not exhibit heterogeneous freezing in sufficient quantity (i.e., a low number of ice crystals were observed) to constitute a signal, and hence, their results were also presented as upper limits. Mahrt et al. (2018) observed no evidence of immersion/condensation freezing above water saturation using a continuous flow diffusion chamber (CFDC), regardless of particle size or physicochemical properties, based on measurements of commercially available soots and laboratory-generated propane-based soots. Kanji et al. (2020) made similar measurements to that of Mahrt et al. (2018), demonstrating that different soot/BC types generated from synthetic and fossil fuels at atmospherically relevant size do not effectively nucleate ice in their system. Vergara-Temprado et al. (2018) investigated the relationship between INP concentrations and BC produced

heterogeneous freezing in sufficient quantity (i.e., a low number of ice crystals were observed) to constitute a signal, and hence, their results were also presented as upper limits. Mahrt et al. (2018) observed no evidence of immersion/condensation freezing above water saturation using a continuous flow diffusion chamber (CFDC), regardless of particle size or physiochemical properties, based on measurements of commercially available soots and laboratory-generated propane-based soots. Kanji et al. (2020) made similar measurements to that of Mahrt et al. (2018), demonstrating that different soot/BC types generated from synthetic and fossil fuels at atmospherically relevant size do not effectively nucleate ice in their system. Vergara-Temprado et al. (2018) investigated the relationship between INP concentrations and BC produced from two different fuel sources, *n*-decane and eugenol, by immersing particles in microliter volume droplets. No freezing was observed at temperatures above those in the control experiments. The authors were able to derive limiting values of the effectiveness of BC's ability to nucleate ice and suggested that, even given the copious amounts of BC in the atmosphere, BC does not compete with other INP types, such as mineral dust.

Far fewer studies of ice nucleation by combustion ashes have been performed, but it has been shown that ashes from multiple fuels nucleate ice with varying effectiveness. However, the amounts of ash in the atmosphere are poorly constrained, and it is therefore difficult to determine their importance (Grawe et al., 2016, 2018; Umo et al., 2015, 2019).

Overall, the picture of whether combustion aerosol is important for ice nucleation is far from clear. The fuel burned and the combustion conditions play important roles in controlling the properties of the ash and aerosol produced; hence, it might be expected that the ice-nucleating properties are also variable (Levin et al., 2016; McCluskey et al., 2014; Petters et al., 2009). Hence, a fruitful approach may be to target real-world combustion events that produce combustion aerosol from a range of fuels and combustion conditions in order to assess whether these events yield elevated (or reduced) INP concentrations.

In this study, we made measurements during a combustion aerosol event associated with the Bonfire Night, or Guy Fawkes Night, festivities that are widely celebrated annually on and around the 5 November across the United Kingdom and involve the burning of bonfires and setting off of fireworks. Measurements were made over one day and night in 2016 (during the day on 5 November 2016 and into the early hours of the following morning) and over two days and nights in 2017 (4 and 5 November 2017). During these events, the bonfires consist of a range of combustible materials. These fuels include waste wood, some of which is untreated while some is treated with a range of preservatives and paints; garden waste, including branches, leaves, and stems of plants, with varying water content; and household waste from old newspapers and cardboard to plastic and rubber items. These bonfires produce large quantities of combustion aerosol that can be observed from space (Pope et al., 2016). Fireworks also produce combustion aerosol and potentially release aerosol containing trace metals into the atmosphere (Lin, 2016). Previous studies have shown increases in aerosol concentration during cultural celebrations of a similar nature (Ardon-Dryer & Levin, 2014; Moreno et al., 2007; Singh et al., 2015), with the aerosol produced during these events containing a mixture of BC, unburnt hydrocarbons, combustion ashes, and aerosols composed of metals and sulfates that are associated with fireworks (Jiang et al., 2015; Reyes-Villegas et al., 2018). Another factor that can affect the aerosol produced is the temperature of the bonfires, with typical bonfires being between 600°C and 1100°C when lit. Given that atmospheric aerosol and BC concentrations are well known to be significantly enhanced during Bonfire Night, we would therefore anticipate an enhancement in ambient INP concentrations if the combustion aerosols produced were effective INPs.

2. Methods

2.1. Sampling Site, Meteorological Conditions, and Air Mass Origins

Aerosol sampling was performed on the balcony of the School of Earth and Environment building which is approximately 15 m above surface level. This measuring site was chosen in part because it is some distance from any point sources of combustion aerosol. The site was more than ~0.5 km from any specific bonfires or firework displays in order to provide a representative overview of combustion aerosol emitted across the city during Bonfire Night, and also being situated in the center of the Campus it is around 0.3 km from any major roads, suburban areas, and other typical urban combustion sources. Bonfire Night is typically celebrated with small fires and fireworks in private gardens as well as more significant fires and firework displays at organized events at designated sites in, for example, suburban parks. The vast majority of the festivities are in the suburbs and less densely built-up areas; hence, the University of Leeds campus (53.8067°N, 1.5550°W), which is located close to Leeds city center, was chosen a sampling location. A map indicating the sampling point and the surrounding urban location can be seen in Supporting Information (SI) Figures S1a and S1b, respectively.

Air mass back trajectories corresponding to the INP sampling periods, determined using HYSPLIT (Stein et al., 2015), are shown in the SI (Figures S2–S4). The evening of 5 November 2016 (16:00–01:00) was characterized with moderately strong northerly winds (2.9 m s⁻¹ average speed), a lack of precipitation, and temperatures ranging from 3.3°C to 7.3°C. The air masses uniformly came from the North of the United Kingdom, the North Sea, and Scandinavia. The sampling period of 4 November 2017 (15:30–23:30) saw north-westerly winds (1.3 m s⁻¹ average speed), no precipitation, and temperatures ranging between 6.1°C and 10.3°C. The air masses uniformly came across the North Atlantic Ocean, having been in the Canadian Arctic 120 h previously. The sampling period of 5 November 2017 (16:00–02:30) had similar characteristics

to that of the previous evening, with the air masses having traveled uniformly over the North Atlantic Ocean from the Canadian Arctic. Wind speed was at an average of 0.9 m s^{-1} , no precipitation was observed, and temperatures ranged between 2.3°C and 8.6°C .

The fact that the air mass back trajectories were uniform in origin during each of the sampling periods, were all free from precipitation, and saw similar temperature variation allowed for comparison between sampling periods. Hence, any changes in the INP concentration might be more readily attributed to Bonfire Night combustion aerosol. Given that the majority of the combustion aerosol we sampled would have come from the suburbs of the city of Leeds, that is, from about 0.5 to $\sim 10 \text{ km}$ away, this corresponds to a time between emission and sampling of between 3 and 60 min for the 5 November 2016 and 15 to 180 min for the lower wind day of 5 November 2017. A recent review of biomass burning (biomass burning is not entirely representative of bonfire night, but there are some notable similarities, i.e., wood burning) plumes suggests a possible correlation between biomass burning plumes where the aerosol has been aged for less than 5 h (which would include all our measurements) and a PM mass increase; however, it is not clear if this correlation is real due to a low number of data points (Hodshire et al., 2019). The same review showed a distinct positive correlation between oxidation (based on organic aerosol composition markers) and aging. As INPs are not necessarily related to bulk particle properties, it remains unclear how any of these factors may affect the ice-nucleating ability of the combustion aerosol we sampled.

2.2. Aerosol Sampling

Aerosol was sampled onto $0.4\text{-}\mu\text{m}$ pore size track-etched membrane polycarbonate filters (Nuclepore, Whatman) using an omnidirectional ambient air particulate sampler (BGI PQ100, Mesa Laboratories Inc.) designed to US Environmental Protection Agency (EPA) regulations (designation no. RFPS-1298-124). The PQ100 had a PM_{10} cutoff and sampled at a volumetric flow rate of 16.7 L min^{-1} (i.e., $1 \text{ m}^3 \text{ h}^{-1}$). Despite the pore size in the filters being $0.4 \mu\text{m}$, the filters retain a high collection efficiency for particles much smaller than this through a variety of mechanisms, as shown in various studies (Lindsley, 2014; Soo et al., 2016). Based on data from these studies, the minimum collection efficiency of the filters occurs at 30 nm, with the efficiency being 85%. The collection efficiency was much higher over the rest of the aerosol size distribution (approaching 100%). The filter samples in this study were collected approximately hourly in order to provide sufficient temporal resolution to track the evolution of the combustion events and also to collect enough aerosol to obtain detectable INP signals. Sampling times were chosen in order to encompass the conditions before and after the celebrations started, and the corresponding rise and fall in aerosol concentrations. Table S1 in section 5 of the SI shows the sampling time and the volume of collected air of each filter.

2.3. INP Analysis

After sampling, each filter was washed with 5 ml of purified water ($18.2 \text{ M}\Omega \text{ cm}$ at 25°C , $0.22 \mu\text{m}$ filtered) for 1 h on a rotary mixer (Clifton RM-1, Nickel-Electro Ltd.) operated at 0.5 Hz, similar to previously described methods (Hill et al., 2014; O'Sullivan et al., 2018), in order to generate a suspension of the collected aerosol particles. The suspensions were then subjected to immersion mode freezing analysis using three different but complementary cold stage techniques to quantify ambient INP concentrations over more than 6 orders of magnitude ($\sim 10^{-3}$ to 10^3 L^{-1} of air), covering a key range of atmospheric relevance. Each cold stage instrument uses a different droplet volume during the freezing experiment, and the size of the droplet is directly proportional to the freezing temperature when measuring the same species of INP. Simply, the greater the droplet volume, the more likely that more active (in terms of freezing temperature) INPs will be present (Vali, 1971).

The InfraRed Nucleation by Immersed Particles Instrument (IR-NIPI) is a large volume drop freeze assay that employs a 96-multiwell plate containing $50\text{-}\mu\text{l}$ aliquots of sample, which is placed upon a cold plate. The operation of the IR-NIPI is described in Harrison et al. (2018), wherein the multiwell plate containing the droplet array is cooled at 1°C min^{-1} until all of the droplets are frozen. This cooling process is monitored by an infrared camera, and a time lapse of thermal images is taken. When a droplet freezes, it releases heat

proportional to the freezing temperature when measuring the same species of INP. Simply, the greater the droplet volume, the more likely that more active (in terms of freezing temperature) INPs will be present (Vali, 1971).

The InfraRed Nucleation by Immersed Particles Instrument (IR-NIPI) is a large volume drop freeze assay that employs a 96-multiwell plate containing 50- μ l aliquots of sample, which is placed upon a cold plate. The operation of the IR-NIPI is described in Harrison et al. (2018), wherein the multiwell plate containing the droplet array is cooled at $1^{\circ}\text{C min}^{-1}$ until all of the droplets are frozen. This cooling process is monitored by an infrared camera, and a time lapse of thermal images is taken. When a droplet freezes, it releases heat energy that is detected by the IR camera, which is used to determine the temperature at which the droplet froze. The microliter Nucleation by Immersed Particle Instrument (μ l-NIPI) (Whale, Murray, et al., 2015) involves pipetting ~50 droplets of 1- μ l volume onto a hydrophobic glass slide that is positioned on a cold stage. The droplets are frozen upon cooling the stage to -40°C at $1^{\circ}\text{C min}^{-1}$, with the freezing

temperature for each droplet recorded via a digital camera. Finally, a microfluidic platform was employed to generate 278 ± 66 -pl droplets of aqueous sample for analysis using a Peltier element-based version of the picoliter Nucleation by Immersed Particle Instrument (pl-NIPI) technique (Tarn et al., 2018), which had previously comprised of a nebulizer for droplet production and a liquid nitrogen-based cold stage for cooling (O'Sullivan et al., 2014). Water-in-oil droplets were generated on-chip and collected off-chip, then cooled to -40°C at $1^{\circ}\text{C min}^{-1}$ on the Peltier element-based cold stage, with freezing events recorded using a digital camera. The fabrication and operation of the microfluidic chip and cold stage are described by Tarn et al. (2018). Briefly, the microfluidic chip featured a flow-focusing droplet generation structure that was fabricated in polydimethylsiloxane (PDMS) using standard soft lithography procedures, allowing water-in-oil droplets to be produced using a fluorinated oil phase (3M™ Novec™ 7500 oil containing 2% w/w Pico-Surf™ 1 surfactant, Sphere Fluidics, UK). All collected aerosol samples were analyzed using the $\mu\text{l-NIPI}$, but only selected samples were further analyzed using the IR-NIPI and the microfluidic pl-NIPI. Control experiments were performed using handling blanks by putting a filter through the entire experimental process apart from having air sampled through it.

The number of INPs per unit volume of sampled air, $[\text{INP}]_T$, was calculated from the immersion mode freezing analysis using Equation 1, adapted from Vali (1971):

$$[\text{INP}]_T = \frac{-\ln(1 - f_{\text{ice}}(T))}{V_d} \cdot \frac{V_w}{V_a} \quad (1)$$

where $f_{\text{ice}}(T)$ is the fraction of droplets frozen at temperature T , V_d is the droplet volume, V_w is the volume of water used to wash particles off the filter (i.e., 5 ml), and V_a is the volume of air sampled through the filter. V_d varies between different NIPI instruments as described above, and the details of V_a for each sample are provided in SI Table S1. In order to estimate the uncertainty in the INP concentrations, we used a method that accounts for the randomness of the distribution of ice-nucleation active sites across the droplets in the experiment and also accounts for the counting uncertainty associated with detecting ice-nucleation active sites within a population (Harrison et al., 2016).

2.4. Online Aerosol Monitoring

Aerosol size distributions and BC mass loading were measured throughout the event, allowing for the comparison of INP concentrations with varying aerosol and BC loadings. In order to measure particle size distributions, an aerodynamic particle sizer (APS; Model 3321, TSI Inc.) was used during all three sampling periods, while a scanning mobility particle sizer (SMPS; Model 3936, TSI Inc.) was used in 2016 only. Unfortunately, the SMPS system was not operational in 2017. The APS was sensitive to a particle diameter distribution in the range of 0.542–19.81 μm (aerodynamic), whereas the SMPS had an effective range of 17.5–552.3 nm (electrical mobility). A BC aethalometer (microAeth AE51, Aethlabs) was used to measure BC mass concentrations (ng m^{-3}) with a specific attenuation of $12.5 \text{ m}^2 \text{ g}^{-1}$ applied to convert optical attenuation into mass. Comparisons of the AE51 (single wavelength, 880 nm) to the widely used AE31 (multi-wavelength) aethalometer can be found in the literature and showed that the measured BC mass concentrations agreed to within 14% (Cheng & Lin, 2013). PM_{10} concentration data were also obtained from a Department for Environment, Food and Rural Affairs (DEFRA) station based in Leeds city center (approximately 1 km away from the sampling site).

2.5. Scanning Electron Microscopy

Further to the aerosol instrumentation, several filter samples were taken in parallel to those collected for INP measurements so that scanning electron microscopy (SEM) could then be employed to obtain chemical composition and size distributions of the aerosol particles trapped on the filters using the technique described by Sanchez-Marroquin et al. (2019). The filters collected for SEM analysis had similar time resolutions to those used for INP analysis but were not measured at exactly the same time. In brief, the SEM analysis was performed using a Tescan Vega3 XM SEM fitted with an X-max 150 SDD energy-dispersive X-ray spectroscopy (EDS) system and controlled by AZtec 3.3 software with a particle analysis expansion (AZtecFeature). Filter samples were coated with 30 nm of iridium prior to analysis, and the microscope was operated at 20 keV and a working distance of 15 mm using the secondary electron detector. The particles were scanned in different areas across the filter, using two different magnifications: approximately 5,000X

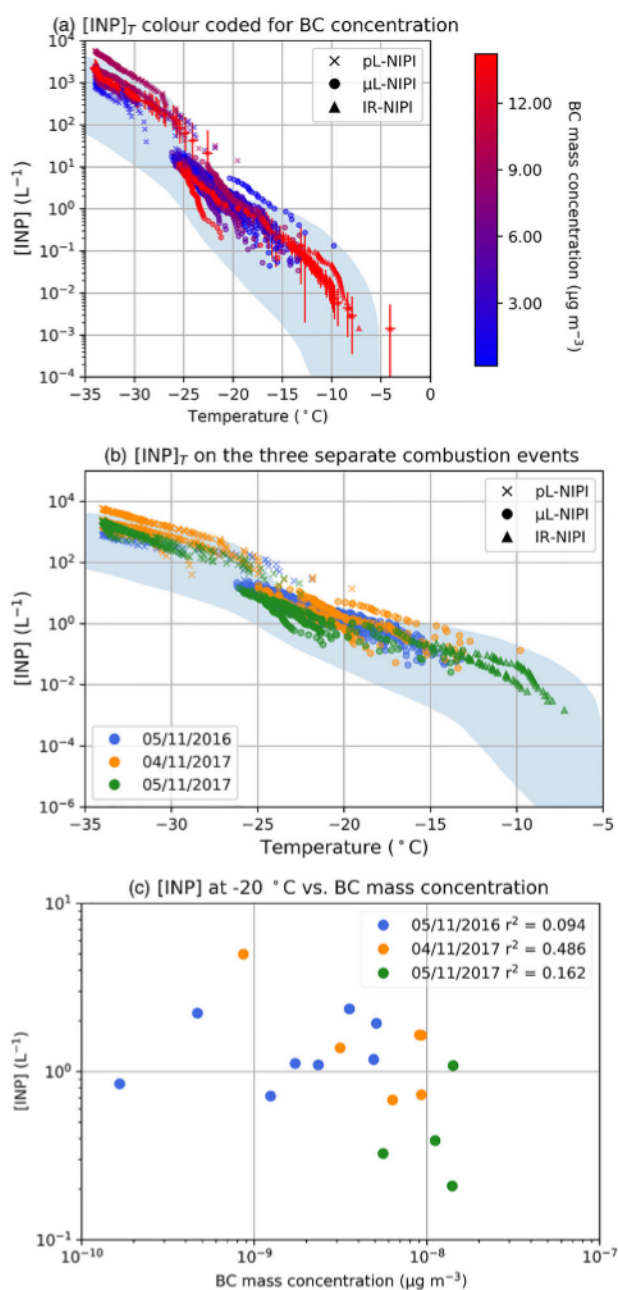


Figure 1. Atmospheric INP concentrations measured during the three sampling periods and their relationship to black carbon (BC). (a) Atmospheric [INP]_T spectra corresponding to each filter sample collected during three combustion aerosol events. The IR-NIPI obtained measurements from about -8°C to -15°C (for a small number of samples), the μL -NIPI in the range -15°C to -25°C (for all samples), and the pL-NIPI in the range -25°C to -34°C (for a selection of samples). The blue envelope is based upon the range of observed INP concentrations in midlatitude terrestrial environments (Petters & Wright, 2015). The [INP]_T spectra are color coded according to the mean BC mass concentration during the run sample time, as measured by the aethalometer. The first sample taken on 5 November 2017 is not included as the aethalometer was only operating for part of the sampling time. (b) The same

for particles with a diameter greater than $0.3\ \mu\text{m}$ and approximately 1,500X for particles greater than $1\ \mu\text{m}$ in diameter. The particle identification was performed based on the relative brightness with respect to the background. The equivalent circular diameter of each particle (defined as $(4A_p/\pi)^{0.5}$, where A_p is the cross-sectional area of the particle) was extracted from each image of the filter to obtain a size distribution. In addition, EDS was performed in the center of some of the particles of each image (50,000 counts per particle), from which the measured spectra were used to calculate elemental weight percentages using the AZtec software. In total, more than 4,000 particles per filter were analyzed. Using these elemental weight percentages, particles were then categorized according to their composition using a sequential algorithm in the AZtecFeature software. The software distinguished aerosol particles primarily based on their chemical composition and assigned particles to a particular category^{OBJ} (Sanchez-Marroquin et al., 2019) and discussed in section 3 of the SI. In this work, typically $<5\%$ of particles in each sample were not classified by the scheme and are labeled as “Others” in the results.

3. Results and Discussion

3.1. Atmospheric INP Measurements

The atmospheric INP concentrations as a function of temperature ([INP]_T) for the three nights are presented in Figure 1a, with the [INP]_T spectra color coded for BC concentration. Measurements were made over 6 orders of magnitude, from 1.5×10^{-3} to 4×10^3 INP L⁻¹, using the three different cold stage devices (Figure 1a). The maximum variation in INP concentration at a given temperature throughout the [INP]_T spectra in Figure 1a was approximately 1.5 orders of magnitude. The spectra on each day were similar to one another during the three sampling periods over the 2 years, as shown in Figure 1b. Fraction frozen curves for all of the spectra, from which the INP concentration plots were derived, are shown in the SI (Figure S6) alongside those of the handling blanks.

Figure 1a also shows the range of INP concentrations reported for locations across the terrestrial northern hemisphere midlatitudes based on the INP content of precipitation samples (Petters & Wright, 2015). The majority of the measured INP concentrations fell within the range defined by Petters and Wright (2015), with a small fraction being slightly above this range between temperatures of -15°C and -22°C . This showed that, during the majority of the measurement periods, INP concentrations fell within a typical range for the terrestrial midlatitudes.

The color coded [INP]_T spectra in Figure 1a indicate that there was no correlation of BC with INP concentration in the measured temperature regime. To further demonstrate the lack of [INP]_T dependence on BC (a tracer for combustion aerosol), Figure 1c shows a correlation plot comparing the change in [INP]_T at -20°C (chosen as we have the greatest number of data points at this temperature)

[INP]_T spectra corresponding to each filter sample collected during three combustion aerosol events. The IR-NIPI obtained measurements from about -8°C to -15°C (for a small number of samples), the $\mu\text{l-NIPI}$ in the range -15°C to -25°C (for all samples), and the pl-NIPI in the range -25°C to -34°C (for a selection of samples). The blue envelope is based upon the range of observed INP concentrations in midlatitude terrestrial environments (Petters & Wright, 2015). The [INP]_T spectra are color coded according to the mean BC mass concentration during the run sample time, as measured by the aethalometer. The first sample taken on 5 November 2017 is not included as the aethalometer was only operating for part of the sampling time. (b) The same plot as in (a) but in which the [INP]_T are color coded by day. (c) A correlation plot showing [INP] at -20°C versus BC mass concentration, color coded by day. Error bars are shown on a selection of spectra on each cold stage device.

measurement periods, INP concentrations fell within a typical range for the terrestrial midlatitudes. The color coded [INP]_T spectra in Figure 1a indicate that there was no correlation of BC with INP concentration in the measured temperature regime. To further demonstrate the lack of [INP]_T dependence on BC (a tracer for combustion aerosol), Figure 1c shows a correlation plot comparing the change in [INP]_T at -20°C (chosen as we have the greatest number of data points at this temperature) with the change in mean BC mass concentration throughout the sampling duration for different samples. The relatively low R^2 values on each day indicate that the concentrations of INP and BC were not correlated.

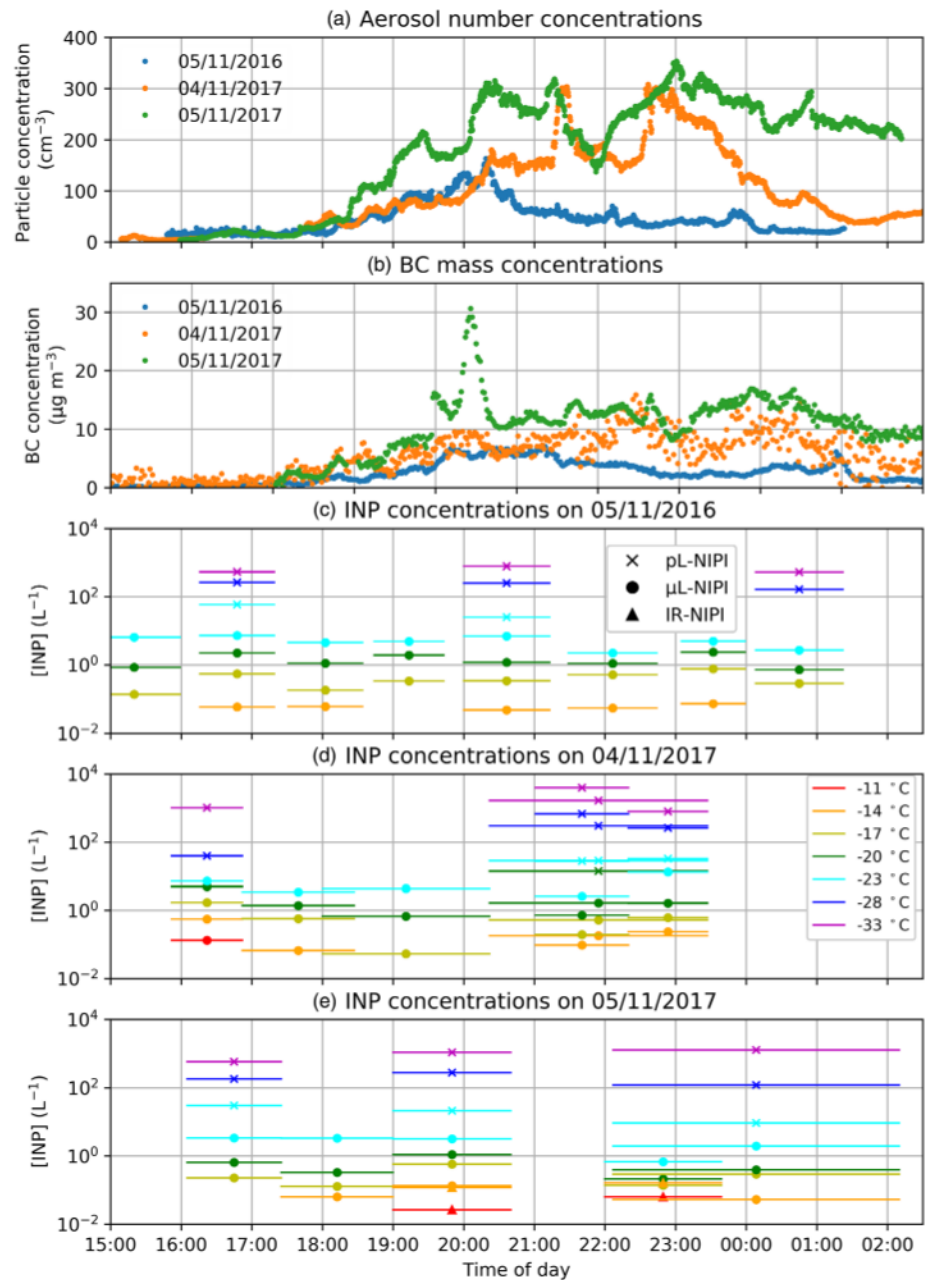


Figure 2. Aerosol number concentration, black carbon (BC) mass concentration, and INP concentrations as a function of time throughout each of the three combustion events. (a) The concentration of aerosol particles measured using an APS (0.542–19.81 μm of aerodynamic diameter). (b) The BC concentration measured using a BC aethalometer. (c–e) INP concentrations at different temperatures for 5 November 2016, 4 November 2017, and 5 November 2017, respectively. Points are plotted on the x axis at the midpoint of the sampling time. Shape markers indicate the midpoint of a run, with horizontal lines either side showing the entire sampling period.

3.2. Time Evolution of Aerosol and INP Concentrations

In Figure 2, we compare the time evolution of $[\text{INP}]_T$ with a measure of aerosol loading and BC mass during the three distinct combustion events. Relatively low aerosol concentrations (measured with an APS; $\sim 0.5\text{--}20\ \mu\text{m}$ of particle diameter range) were observed until around 18:00 on all three sampling days, before the majority of Bonfire Night celebrations began (Figure 2a). At around this time on each day, aerosol concentrations began to rise and increased by over 1 order of magnitude in 2016 and 2 orders of magnitude over

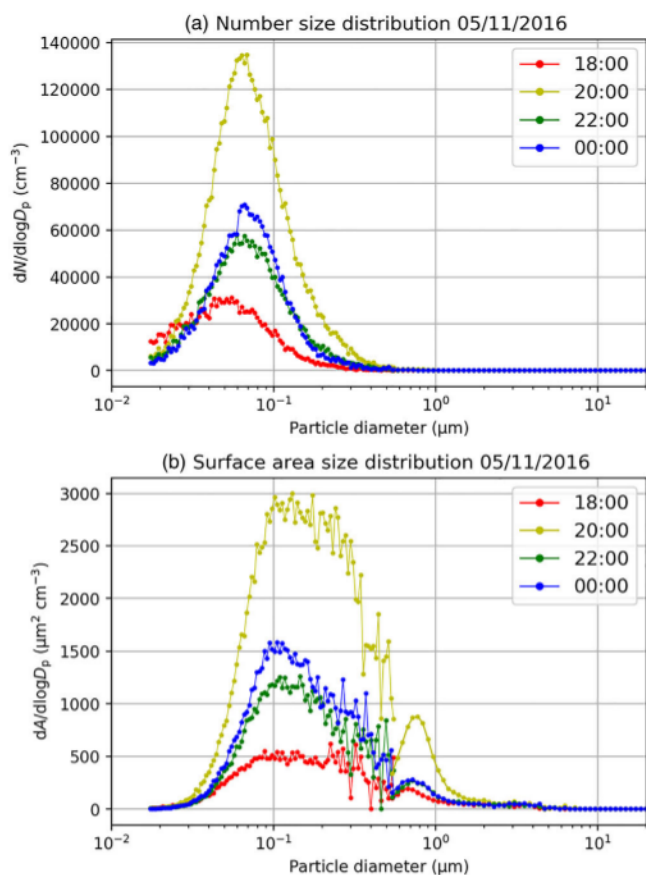


Figure 3. Size distribution of atmospheric aerosol particle populations measured on 5 November 2016 in terms of (a) number concentration and (b) surface area concentration. Size distributions are shown at 2-h increments between 18:00 and 00:00. The x axis is presented in volume equivalent spherical diameter (D_p). The electrical mobility data from the SMPS and aerodynamic data from the APS were merged to produce a volume equivalent diameter. This was performed using the method described by Möhler et al. (2008).

November 2017, BC concentrations peaked at approximately 21:30 and again at 22:45, reaching concentrations of $15 \mu\text{g m}^{-3}$, which mirrored the corresponding aerosol concentration shown in Figure 2a. Thereafter, the BC concentrations began to subside but remained significantly elevated when compared to pre-event concentrations. The sampling event on 5 November 2017 saw an extreme peak at 19:30, with BC concentrations measured at $31 \mu\text{g m}^{-3}$, before subsiding to similar levels to those observed on 4 November 2017. Similarly, to the aerosol concentrations, the 4 November 2017 BC concentrations remained elevated into the early hours of the next day.

The INP concentrations at a series of temperatures for each combustion event are shown in Figures 2c–2e on the same time scale as the aerosol and BC measurements. As can be seen, despite large increases in aerosol concentration and BC from 18:00 onward (Figures 2a and 2b), no corresponding increases in INP concentrations were observed outside of the random run-to-run variability, that is, about a factor of 2 (based on the standard deviation of $[\text{INP}]_T$; see Table S2). The low variability in $[\text{INP}]_T$ is consistent with the back trajectory analyses (Figures S2–S4 in the SI), which revealed fortuitous sampling conditions in which the air mass origins exhibited very little variability within each sampling period. Hence, these air masses were exposed to similar INP sources during their transport within each sampling period. This was fortunate, because it

both days in 2017. During the 5 November 2016 sampling event, the SMPS (~18–550 nm of particle diameter range) also measured an increase in total aerosol number concentration of approximately an order of magnitude (SI Figure S8). The full size distribution for a selection of times is shown for 5 November 2016 in Figure 3, with APS size distributions for both 2017 events shown in the SI (Figure S9). In Figure S9f (5 November 2017) a large increase in coarse mode aerosol surface can be seen in the 00:00 size distribution, which may correspond to the increase in number concentration seen during that event after 22:00. These number and surface area distributions demonstrate that the aerosol concentration increased across the fine and coarse modes over the course of the combustion event. On 5 November 2016, aerosol concentrations returned to relatively low levels once the main celebrations had concluded (approximately 22:00). However, for the sampling periods on 4 and 5 November 2017, the high concentrations persisted until the earlier hours of the following morning, with the 5 November 2017 aerosol concentrations remaining well above background levels until measurements were stopped shortly after 02:00 on 6 November 2017. This is consistent with the greater wind speeds on the evening of the 5 November 2016, which resulted in the polluted air being swept away and replaced with cleaner air. A plot of PM_{10} concentrations from a Leeds city center air monitoring station for each sampling day is also shown in the SI (Figure S11). The trends show qualitative agreement between the APS data from the measurement site and the PM_{10} monitoring station, indicating that the increases in aerosol concentration during the combustion events were representative of a wider area across the city.

The variation in BC concentrations throughout the three events is shown in Figure 2b. On each of the sampling days, BC began to substantially increase at approximately 18:00, peaking at $5\text{--}30 \mu\text{g m}^{-3}$ and remaining elevated for several hours. During 5 November 2016, BC concentrations peaked between 19:00 and 20:00 and then decreased throughout the remainder of the sampling period. On 4

The INP concentrations at a series of temperatures for each combustion event are shown in Figures 2c–2e on the same time scale as the aerosol and BC measurements. As can be seen, despite large increases in aerosol concentration and BC from 18:00 onward (Figures 2a and 2b), no corresponding increases in INP concentrations were observed outside of the random run-to-run variability, that is, about a factor of 2 (based on the standard deviation of $[\text{INP}]_T$; see Table S2). The low variability in $[\text{INP}]_T$ is consistent with the back trajectory analyses (Figures S2–S4 in the SI), which revealed fortuitous sampling conditions in which the air mass origins exhibited very little variability within each sampling period. Hence, these air masses were exposed to similar INP sources during their transport within each sampling period. This was fortunate, because it allowed us to make a direct comparison of $[\text{INP}]_T$ spectra between peak pollution times and prior to the events. The lack of dependency of INP concentration on aerosol loading is particularly striking between about 19:00 and 21:00 on 5 November 2016, 21:00 and 22:00 on 4 November 2017, and 19:00 and 20:00 on 5 November 2017, as these time periods showed a peak in terms of aerosol and BC concentrations. This

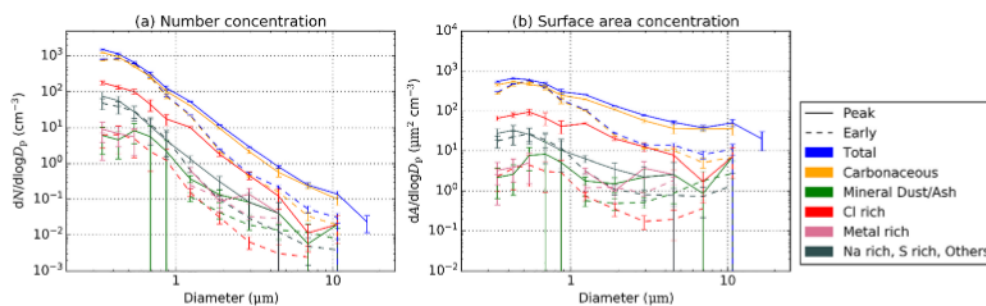


Figure 4. Composition of particles collected on the early (5 November 2017, 16:05–17:25) and peak (5 November 2017, 00:00–00:45) filters in terms of (a) number concentration and (b) surface area. The errors were calculated using Poisson counting statistics. These plots were generated using SEM-EDS analysis.

suggests that the aerosol emitted during these combustion events did not substantially contribute to the atmospheric INP population. As discussed above, the INP concentrations observed in Leeds were typical of midlatitude INP concentrations (see the Petters & Wright, 2015, data in Figure 1), and thus, the concentrations of ambient INPs were not unusually high; hence, an increase in activity due to the presence of a new source of INPs would likely have been noticeable. It would be interesting to conduct a similar series of experiments in a very low INP environment, such as a location influenced directly by remote marine air (DeMott et al., 2016; McCluskey et al., 2018), where any ice-nucleating ability of combustion aerosol might become apparent.

3.3. Aerosol Particle Characterization by SEM-EDS

SEM-EDS was used to measure the chemical composition of two filter samples collected on 5 November 2017 (16:05–17:25, referred to as “early”; 00:00–00:45, referred to as “peak loading”) using the methodology defined previously (Sanchez-Marroquin et al., 2019). Figure 4 shows the size distribution in terms of particle number concentration and particle surface area concentration for both filters, broken down into groups based on their chemical composition. For both filters, the aerosol samples were dominated by carbonaceous particles, which are consistent with organic aerosol, primary biogenic particles, or BC. In addition, there were significant contributions of mineral dust and/or ash (particles in the categories “Si only,” “Si rich,” “Al-Si rich,” and “Ca rich”), and particles dominated by metal signals, mainly Fe and Al (“Metal rich”), which could have a crustal or anthropogenic origin. In addition, there was also a significant fraction of “Cl rich” particles. Particles in this category were dominated by the presence of Cl (and sometimes K) but not Na, so they were not compatible with sea spray aerosol (which appear in the “Na rich” category) (Sanchez-Marroquin et al., 2019). These Cl-rich particles may originate from fireworks set off during the festivities, which often contain metal chlorides and some potassium compounds in the form of perchlorates or chlorates, among many other components (Li et al., 2017; Lin, 2016; Liu et al., 1997). Crespo et al. (2012), for example, reported strong increases in Cl and K concentrations in the fine aerosol fraction, as well as a significant increase in the coarse fraction, during a pyrotechnic event. Further, a study of 41 wildfires in the United States showed that increased concentrations of Cl and K are also associated with wildfires (Schlosser et al., 2017), suggesting that the observed increase in Cl- and K-rich particles during the sampling event may also be due to the burning of wood and other biomass on bonfires.

In terms of changes between the early and peak event filters, a clear increase can be seen in the concentration of carbonaceous particles, particularly those above 1- μm diameter that most likely resulted from incomplete combustion. A clear increase in Cl-containing aerosol was observed that was probably associated with pyrotechnics, although it could potentially be attributed to biomass burning. An increase in mineral dust/ash particles was also observed across all sizes, which may be related to emissions of combustion ash particles; this is discussed further below. However, the measured surface areas for each filter in the mineral dust/ash category were within error of each other ($6 \pm 4 \mu\text{m}^2 \text{cm}^{-3}$ for the peak filter and $1.3 \pm 0.7 \mu\text{m}^2 \text{cm}^{-3}$ for the early filter). Overall, the chemistry of the aerosol particle population changed in a manner consistent with what we would qualitatively expect over Bonfire Night. Section 5 of the SI shows images of a filter before and after sampling to give an example of the aerosol loading (Figure S7).

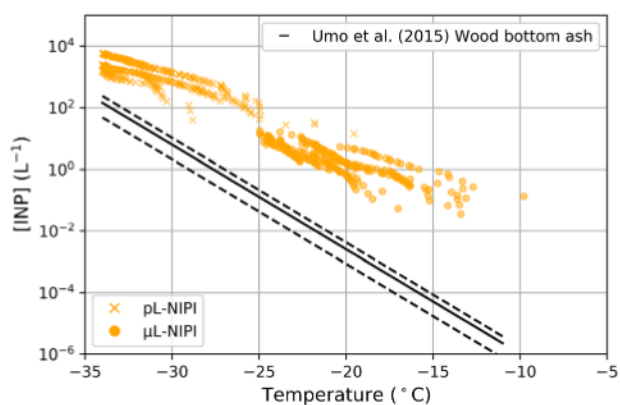


Figure 5. Comparison of a predicted upper limit $[INP]_T$ spectrum for combustion ash compared with measured $[INP]_T$ spectra. The $[INP]_T$ spectrum for ash was based on the measured surface area of mineral dust/ash from the SEM-EDS analysis, assuming that all this material was ash, and the parameterization for wood bottom ash (Umo et al., 2015). The dashed lines represent uncertainties in $[INP]_T$ based upon the uncertainties in the SEM-derived surface area of mineral dust/ash. The $[INP]_T$ measurements and the SEM filters were collected on 4 November 2017.

3.4. Contribution of Atmospheric INP by Combustion Ash and Mineral Dust

The difference measured between the early and peak filters in the mineral dust/ash category from the SEM-EDS analysis is potentially explained by an increase in ash lofted from bonfires as part of the celebration. In order to quantify the potential contribution of ash to the atmospheric INP concentration, the SEM-EDS measurement for the surface area concentration of mineral dust/ash in the atmosphere from the “peak” filter ($6 \pm 4 \mu\text{m}^2 \text{cm}^{-3}$) was taken as an upper limit to the ash surface area contributed by the combustion event. We used this surface area measurement with the ice-nucleation activity parameterization for wood bottom ash from Umo et al. (2015) to calculate an upper limit to the potential contribution of ash to the atmospheric INP concentration. Coal fly ash was found to be more active than bottom ashes (Grawe et al., 2018; Umo et al., 2015) but is probably not relevant for Bonfire Night emissions. Umo et al. (2015) derived their n_s parameterization using a surface area derived from gas adsorption measurements, which generally produce a larger surface area than the geometric surface area. Hence, this may produce an estimate of INP concentration which is biased low, but the bias is most likely not large enough to change the conclusions below. It should also be noted

that bottom ash samples are not necessarily an ideal proxy for combustion ash aerosol produced on Bonfire Night, but the activity of the ash component of combustion aerosol has not been measured. The ice-nucleating activity of combustion ash is thought to be related to the mineral components of this material (Grawe et al., 2018; Umo et al., 2015).

Across the entire temperature range that the Umo et al. (2015) parameterization is valid for (-11°C to -34°C), the upper limit to the contribution of atmospheric INPs is well below the measured $[INP]_T$ (Figure 5). Thus, we conclude that any combustion ash emitted as part of the combustion events would have been a minor component in the overall atmospheric INP burden; this is consistent with the lack of variation of the $[INP]_T$ spectra throughout each event. However, we do not rule out combustion ashes being important in other situations due to the caveats with this analysis (described above).

Based on the SEM-EDS measurements, inferences can be made to the composition of the background INP population. A larger study was carried out by O’Sullivan et al. (2018) in a nearby rural background location. The INP concentrations measured in this study were typical of those measured by O’Sullivan et al. (2018). O’Sullivan et al. (2018) reached the conclusion that the INP concentrations below -18°C in the region were dominated by mineral dust-based INPs, whereas above this temperature biogenic INP could make a significant contribution to the INP burden; this is consistent with the measurements presented in this paper (see discussion in the SI section 8 and Figure S11).

3.5. Limiting Ice-Active Site Surface Density, $n_s(T)$, for BC

The data sets produced during this study provided an opportunity to estimate a limiting value for the ice-nucleating ability of atmospheric BC associated with bonfires and fireworks. Previous estimates of the ice-nucleating ability of BC were based on experiments of laboratory-generated soot samples, whereas in this study we have based our estimate on atmospheric BC that has undergone some degree of processing in the atmosphere and is produced by a range of fuels and combustion conditions. We determined an upper limit to the ice-active site surface density, $n_s(T)$, for BC using the mass concentration of BC shown in Figure 2b, together with INP concentrations measured throughout the combustion events. To estimate an upper limit for the ice-nucleating efficiency of BC, it was assumed that all ice nucleation in the

The data sets produced during this study provided an opportunity to estimate a limiting value for the ice-nucleating ability of atmospheric BC associated with bonfires and fireworks. Previous estimates of the ice-nucleating ability of BC were based on experiments of laboratory-generated soot samples, whereas in this study we have based our estimate on atmospheric BC that has undergone some degree of processing in the atmosphere and is produced by a range of fuels and combustion conditions. We determined an upper limit to the ice-active site surface density, $n_s(T)$, for BC using the mass concentration of BC shown in Figure 2b, together with INP concentrations measured throughout the combustion events. To estimate an upper limit for the ice-nucleating efficiency of BC, it was assumed that all ice nucleation in the samples was due to BC, which is certainly an overestimate but is consistent with the notion of an upper limit. Estimating a surface area of BC allowed $n_s(T)$ values to be calculated using Equation 2 (Connolly et al., 2009):

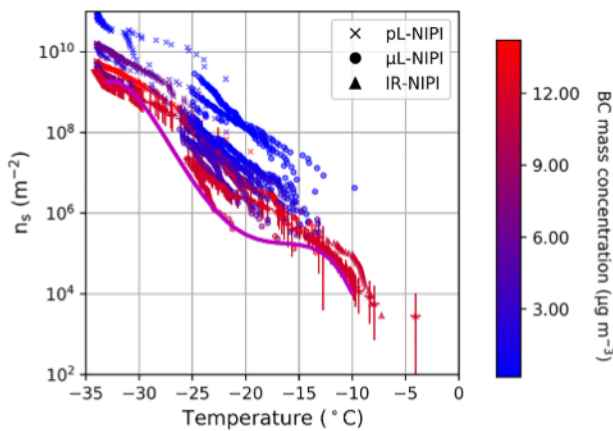


Figure 6. Estimate of the upper limit to the ice-active site surface density, $n_s(T)$, values for BC. Limiting values are estimated from the INP concentration in combination with the BC mass concentration. Triangles, circles, and crosses denote data from the IR-NIPI, μ L-NIPI, and microfluidic pL-NIPI assays, respectively. The lower limit of the data was fitted with a polynomial between -10°C and -33°C , which is shown as a magenta line and used as an upper limit of $n_s(T)$ for BC during Bonfire Night. Error bars are shown on a selection of spectra across the three cold stages.

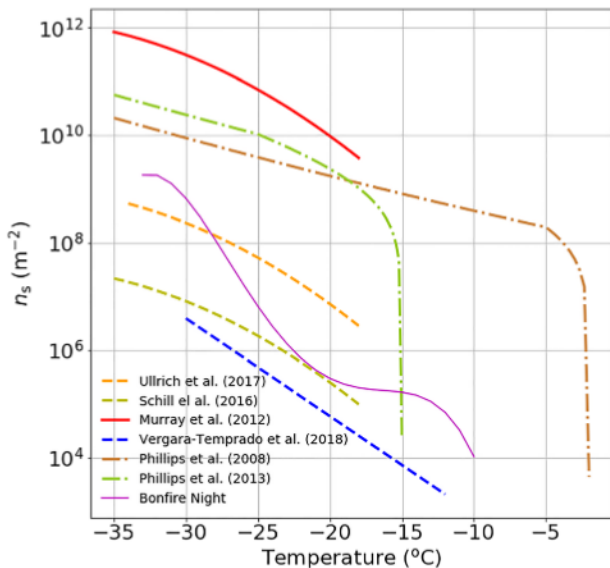


Figure 7. A plot of different BC parameterizations from the literature along with the upper limit to n_s derived in this study of Bonfire Night emissions. The parameterizations from Schill et al. (2016), Ullrich et al. (2017), and Vergara-Temprado et al. (2018) are also upper limits to the activity of BC and were based on laboratory measurements.

$$n_s(T) = \frac{-\ln(1 - f_{\text{ice}}(T))}{A} \quad (2)$$

where $f_{\text{ice}}(T)$ is the cumulative fraction of droplets frozen on cooling to temperature T during the cold stage experiments and A is the surface area of BC per droplet. The estimation of A was determined by assuming that each BC particle was a sphere of 140-nm diameter and had a density of 1.2 g cm^{-3} , based on literature data for BC produced from combustion aerosol (Bond et al., 2013; Gong et al., 2016; Zhang et al., 2016). These assumptions most likely lead to an underestimate in A , which is also consistent with the notion of an upper limit of $n_s(T)$.

We show the limiting $n_s(T)$ values from each sample in Figure 6, color coded to indicate the mean BC mass concentration during the sampling period (as in Figure 1a). The sampling periods with the highest BC concentrations defined the lowest of the limiting values of $n_s(T)$. We fit a polynomial curve to the lowest $n_s(T)$ values, which correspond to the most constrained upper limits we can define (shown by the magenta curve in Figure 7). The equation for the fit is $n_s(T) = \exp(-3.76336674 \times 10^{-4} T^4 - 3.25873608 \times 10^{-2} T^3 - 9.92600404 \times 10^{-1} T^2 - 1.29473300 \times 10^1 T - 4.97896324 \times 10^1)$.

We then compared our fit to literature parameterizations for the n_s of BC in Figure 7. The parameterization from Murray et al. (2012) based on data from DeMott (1990) and Diehl and Mitra (1998) is 3–4 orders of magnitude higher than the limiting value produced from this study in the overlapping temperature range (-18°C to -33°C). Using the Murray et al. (2012) parameterization with the highest BC loading captured by a filter during the Bonfire Night festival in our study would give an $[\text{INP}]_T$ of approximately 105 L^{-1} at -20°C , a value substantially greater than any measured during our campaign. The parameterizations from Phillips et al. (2008) and Phillips et al. (2013) are both below the Murray et al. (2012) parameterization in terms of $n_s(T)$ but are still above our estimate for a limiting $n_s(T)$ value by more than 2 orders of magnitude for nearly the entire overlapping temperature range.

More recent studies of the ice-nucleating ability of BC have, like our Bonfire Night study, produced relatively low upper limits to the ice-nucleating ability of BC (Schill et al., 2016; Ullrich et al., 2017; Vergara-Temprado et al., 2018). These parameterizations are based on data for BC from a number of different fuel sources and combustion conditions, all where no activity was observed. Overall, in the context of the literature data, the limiting value of $n_s(T)$ for BC-based INPs in this study is similar to the values presented by the more recent studies (Schill et al., 2016; Ullrich et al., 2017; Vergara-Temprado et al., 2018), thus contributing further evidence to the growing perception that BC is of secondary importance as an INP in mixed-phase clouds in the terrestrial midlatitudes. However, why the earlier work indicated that BC is an effective ice-nucleating material (Murray et al., 2012; Phillips et al., 2008, 2013) is unclear, and it may be that combustion of some fuels under some conditions can produce BC that is strongly ice active. As mentioned above, elemental carbon in some forms has been shown to nucleate ice effectively (Alstadt et al., 2017; Bai et al., 2019; Whale, Rosillo-Lopez, et al., 2015), but it remains unclear if this highly ice-active form of BC is atmospherically important. Nevertheless, we have shown that BC generated on Bonfire Night from a range of fuels

and combustion conditions has a very low ice-nucleating activity and does not significantly enhance the INP population.

4. Conclusions

INP concentrations were monitored during three similar combustion aerosol events, alongside measurements of aerosol size distribution and BC mass concentration. We took advantage of the annual Bonfire Night celebrations, an annual major bonfire and firework event that takes place across the United Kingdom during the evenings on and around 5 November. We demonstrated that the combustion aerosol generated did not measurably enhance the atmospheric INP concentrations despite a large increase in BC and aerosol concentrations throughout the events. This indicates that BC and other combustion aerosol generated during Bonfire Night are relatively poor INPs and are unable to compete with the background INPs already present in the atmosphere. Using these atmospheric measurements, we derived an upper limit for the ice-active site surface density, $n_s(T)$, of BC, which was consistent with several recent laboratory-derived upper limits. The fact that the BC concentrations peaked at such a high value during our sampling campaign helped to provide a robust constraint to the ice-nucleating ability of BC generated during this type of event. The BC loading during our sampling periods peaked at approximately $31 \mu\text{g m}^{-3}$, with sustained concentrations of $10\text{--}15 \mu\text{g m}^{-3}$ being observed over the course of the combustion aerosol event on the 5 November 2017, which is of a similar magnitude to concentrations observed in some of the most polluted parts of the world (Chen et al., 2016, 2018; Cooke & Wilson, 1996). Concentrations in the midtroposphere are typically well below $0.1 \mu\text{g m}^{-3}$ (Koch et al., 2009; Wofsy, 2011). However, there are some literature studies that have found significant INP activity for BC (DeMott, 1990; Diehl & Mitra, 1998; Levin et al., 2016; Popovicheva et al., 2008), combustion ashes (Grawe et al., 2016; Umo et al., 2015), and combustion aerosol more generally (McCluskey et al., 2014; Petters et al., 2009; Prenni et al., 2009); hence, we cannot discount the possibility that some combination of fuels and combustion conditions might produce more ice-active combustion aerosol. This may be especially true in locations where the background INP loading is relatively low, where even a relatively weak ice-nucleating activity in combustion aerosols may be locally or regionally important for mixed-phase clouds.

Conflict of Interest

The authors declare no conflicts of interest.

Data Availability Statement

The data associated with this paper are openly available from the University of Leeds Data Repository (<https://doi.org/10.5518/809>).

References

- Adachi, K., & Buseck, P. R. (2011). Atmospheric tar balls from biomass burning in Mexico. *Journal of Geophysical Research*, *116*, D05204. <https://doi.org/10.1029/2010JD015102>
- Alstadt, V. J., Dawson, J. N., Losey, D. J., Sihvonen, S. K., & Freedman, M. A. (2017). Heterogeneous freezing of carbon nanotubes: A model system for pore condensation and freezing in the atmosphere. *Journal of Physical Chemistry A*, *121*(42), 8166–8175. <https://doi.org/10.1021/acs.jpca.7b06359>
- Ansmann, A., Tesche, M., Seifert, P., Althausen, D., Engelmann, R., Fruntke, J., et al. (2009). Evolution of the ice phase in tropical alto-cumulus: SAMUM lidar observations over Cape Verde. *Journal of Geophysical Research*, *114*, D17208. <https://doi.org/10.1029/2008JD011659>
- Ardon-Dryer, K., & Levin, Z. (2014). Ground-based measurements of immersion freezing in the eastern Mediterranean. *Atmospheric Chemistry and Physics*, *14*, 5217–5231. <https://doi.org/10.5194/acp-14-5217-2014>
- Bai, G., Gao, D., Liu, Z., Zhou, X., & Wang, J. (2019). Probing the critical nucleus size for ice formation with graphene oxide nanosheets. *Nature*, *576*(7787), 437–441. <https://doi.org/10.1038/s41586-019-1827-6>
- Baustian, K. J., Cziczo, D. J., Wise, M. E., Pratt, K. A., Kulkarni, G., Hallar, A. G., & Tolbert, M. A. (2012). Importance of aerosol composition, mixing state, and morphology for heterogeneous ice nucleation: A combined field and laboratory approach. *Journal of Geophysical Research*, *117*, D06217. <https://doi.org/10.1029/2011JD016784>

Acknowledgments

This work was funded by the European Research Council (H2020 ERC, grants: 648661 MarineIce and 713664 CryoProtect), the Natural Environment Research Council (NERC, grants NE/M010473/1 and NE/L013479/1), the EU-BACCHUS consortium (FP7/2007-797 2013; 603445), and the Engineering and Physical Sciences Research Council (EPSRC, grant EP/M003027/1). Special thanks to Wolfgang Buermann for use of his office during sampling and Franz Conen (University of Basel) for the loan of a Mesa Labs BGI PQ100 sampling unit.

NE/M010473/1 and NE/L013479/1), the EU-BACCHUS consortium (FP7/2007-797 2013; 603445), and the Engineering and Physical Sciences Research Council (EPSRC, grant EP/M003027/1). Special thanks to Wolfgang Buermann for use of his office during sampling and Franz Conen (University of Basel) for the loan of a Mesa Labs BGI PQ100 sampling unit.

- 10.1021/acs.jpca.7b06559
- Ansmann, A., Tesche, M., Seifert, P., Althausen, D., Engelmann, R., Fruntke, J., et al. (2009). Evolution of the ice phase in tropical alto-cumulus: SAMUM lidar observations over Cape Verde. *Journal of Geophysical Research*, *114*, D17208. <https://doi.org/10.1029/2008JD011659>
- Ardon-Dryer, K., & Levin, Z. (2014). Ground-based measurements of immersion freezing in the eastern Mediterranean. *Atmospheric Chemistry and Physics*, *14*, 5217–5231. <https://doi.org/10.5194/acp-14-5217-2014>
- Bai, G., Gao, D., Liu, Z., Zhou, X., & Wang, J. (2019). Probing the critical nucleus size for ice formation with graphene oxide nanosheets. *Nature*, *576*(7787), 437–441. <https://doi.org/10.1038/s41586-019-1827-6>
- Baustian, K. J., Cziczo, D. J., Wise, M. E., Pratt, K. A., Kulkarni, G., Hallar, A. G., & Tolbert, M. A. (2012). Importance of aerosol composition, mixing state, and morphology for heterogeneous ice nucleation: A combined field and laboratory approach. *Journal of Geophysical Research*, *117*, D06217. <https://doi.org/10.1029/2011JD016784>
- Bi, K., McMeeking, G. R., Ding, D. P., Levin, E. J. T., DeMott, P. J., Zhao, D. L., et al. (2019). Measurements of ice nucleating particles in Beijing, China. *Journal of Geophysical Research: Atmospheres*, *124*, 8065–8075. <https://doi.org/10.1029/2019JD030609>
- Bond, T. C., Doherty, S. J., Fahey, D. W., Forster, P. M., Berntsen, T., DeAngelo, B. J., et al. (2013). Bounding the role of black carbon in the climate system: A scientific assessment. *Journal of Geophysical Research: Atmospheres*, *118*, 5380–5552. <https://doi.org/10.1002/jgrd.50171>

- Chen, J., Wu, Z., Augustin-Bauditz, S., Grawe, S., Hartmann, M., Pei, X., et al. (2018). Ice-nucleating particle concentrations unaffected by urban air pollution in Beijing, China. *Atmospheric Chemistry and Physics*, 18(5), 3523–3539. <https://doi.org/10.5194/acp-18-3523-2018>
- Chen, Y., Schleicher, N., Fricker, M., Cen, K., Liu, X., Kaminski, U., et al. (2016). Long-term variation of black carbon and PM 2.5 in Beijing, China with respect to meteorological conditions and governmental measures. *Environmental Pollution*, 212, 269–278. <https://doi.org/10.1016/j.envpol.2016.01.008>
- Cheng, Y.-H., & Lin, M.-H. (2013). Real-time performance of the microAeth® AE51 and the effects of aerosol loading on its measurement results at a traffic site. *Aerosol and Air Quality Research*, 13, 1853–1863. <https://doi.org/10.4209/aaqr.2012.12.0371>
- Connolly, P. J., Möhler, O., Field, P. R., Saathoff, H., Burgess, R., Choularton, T., & Gallagher, M. (2009). Studies of heterogeneous freezing by three different desert dust samples. *Atmospheric Chemistry and Physics*, 9, 2805–2824. Retrieved from. www.atmos-chem-phys.net/9/2805/2009/
- Cooke, W. F., & Wilson, J. J. N. (1996). A global black carbon aerosol model. *Journal of Geophysical Research*, 101(D14), 19,395–19,409. <https://doi.org/10.1029/96JD00671>
- Cozic, J., Mertes, S., Verheggen, B., Cziczo, D. J., Gallavardin, S. J., Walter, S., et al. (2008). Black carbon enrichment in atmospheric ice particle residuals observed in lower tropospheric mixed phase clouds. *Journal of Geophysical Research*, 113, D15209. <https://doi.org/10.1029/2007JD009266>
- Crespo, J., Yubero, E., Nicolás, J. F., Lucarelli, F., Nava, S., Chiari, M., & Calzolari, G. (2012). High-time resolution and size-segregated elemental composition in high-intensity pyrotechnic exposures. *Journal of Hazardous Materials*, 241–242, 82–91. <https://doi.org/10.1016/j.jhazmat.2012.09.017>
- Cziczo, D. J., Froyd, K. D., Hoose, C., Jensen, E. J., Diao, M., Zondlo, M. A., et al. (2013). Clarifying the dominant sources and mechanisms of cirrus cloud formation. *Science*, 340(6138), 1320–1324. <https://doi.org/10.1126/science.1234145>
- de Boer, G., Morrison, H., Shupe, M. D., & Hildner, R. (2011). Evidence of liquid dependent ice nucleation in high-latitude stratiform clouds from surface remote sensors. *Geophysical Research Letters*, 38, L01803. <https://doi.org/10.1029/2010GL046016>
- DeMott, P. J. (1990). An exploratory study of ice nucleation by soot aerosols. *Journal of Applied Meteorology*, 29(10), 1072–1079. [https://doi.org/10.1175/1520-0450\(1990\)029](https://doi.org/10.1175/1520-0450(1990)029)
- DeMott, P. J., Cziczo, D. J., Prenni, A. J., Murphy, D. M., Kreidenweis, S. M., Thomson, D. S., et al. (2003). Measurements of the concentration and composition of nuclei for cirrus formation. *Proceedings of the National Academy of Sciences of the United States of America*, 100(25), 14,655–14,660. <https://doi.org/10.1073/pnas.2532677100>
- DeMott, P. J., Hill, T. C. J., McCluskey, C. S., Prather, K. A., Collins, D. B., Sullivan, R. C., et al. (2016). Sea spray aerosol as a unique source of ice nucleating particles. *Proceedings of the National Academy of Sciences of the United States of America*, 113(21), 5797–5803. <https://doi.org/10.1073/pnas.1514034112>
- DeMott, P. J., Sassen, K., Poellot, M. R., Baumgardner, D., Rogers, D. C., Brooks, S. D., et al. (2003). African dust aerosols as atmospheric ice nuclei. *Geophysical Research Letters*, 30(14), 1732. <https://doi.org/10.1029/2003GL017410>
- Diehl, K., & Mitra, S. K. (1998). A laboratory study of the effects of a kerosene-burner exhaust on ice nucleation and the evaporation rate of ice crystals. *Atmospheric Environment*, 32(18), 3145–3151. [https://doi.org/10.1016/S1352-2310\(97\)00467-6](https://doi.org/10.1016/S1352-2310(97)00467-6)
- Elsasser, M., Busch, C., Orasche, J., Schön, C., Hartmann, H., Schnelle-Kreis, J., & Zimmermann, R. (2013). Dynamic changes of the aerosol composition and concentration during different burning phases of wood combustion. *Energy & Fuels*, 27(8), 4959–4968. <https://doi.org/10.1021/ef400684f>
- Fornea, A. P., Brooks, S. D., Dooley, J. B., & Saha, A. (2009). Heterogeneous freezing of ice on atmospheric aerosols containing ash, soot, and soil. *Journal of Geophysical Research*, 114, D13201. <https://doi.org/10.1029/2009JD011958>
- Gong, X., Zhang, C., Chen, H., Nizkorodov, S. A., Chen, J., & Yang, X. (2016). Size distribution and mixing state of black carbon particles during a heavy air pollution episode in Shanghai. *Atmospheric Chemistry and Physics*, 16(8), 5399–5411. <https://doi.org/10.5194/acp-16-5399-2016>
- Gorbanov, B., Baklanov, A., Kakutkina, N., Windsor, H., & Toumi, R. (2001). Ice nucleation on soot particles. *Journal of Aerosol Science*, 32(2), 199–215. [https://doi.org/10.1016/S0021-8502\(00\)00077-X](https://doi.org/10.1016/S0021-8502(00)00077-X)
- Grawe, S., Augustin-Bauditz, S., Clemen, H. C., Ebert, M., Eriksen Hammer, S., Lubitz, J., et al. (2018). Coal fly ash: Linking immersion freezing behavior and physicochemical particle properties. *Atmospheric Chemistry and Physics*, 18(19), 13,903–13,923. <https://doi.org/10.5194/acp-18-13903-2018>
- Grawe, S., Augustin-Bauditz, S., Hartmann, S., Hellner, L., Pettersson, J. B. C., Prager, A., et al. (2016). The immersion freezing behavior of ash particles from wood and brown coal burning. *Atmospheric Chemistry and Physics*, 16(21), 13,911–13,928. <https://doi.org/10.5194/acp-16-13911-2016>
- Harrison, A. D., Whale, T. F., Carpenter, M. A., Holden, M. A., Neve, L., O'Sullivan, D., et al. (2016). Not all feldspars are equal: A survey of ice nucleating properties across the feldspar group of minerals. *Atmospheric Chemistry and Physics*, 16(17), 10,927–10,940. <https://doi.org/10.5194/acp-16-10927-2016>
- Harrison, A. D., Whale, T. F., Rutledge, R., Lamb, S., Tarn, M. D., Porter, G. C. E., et al. (2018). An instrument for quantifying heterogeneous ice nucleation in multiwell plates using infrared emissions to detect freezing. *Atmospheric Measurement Techniques*, 11(10), 5629–5641. <https://doi.org/10.5194/amt-11-5629-2018>
- Hartmann, M., Blunier, T., Brügger, S. O., Schmale, J., Schwikowski, M., Vogel, A., et al. (2019). Variation of ice nucleating particles in the European Arctic over the last centuries. *Geophysical Research Letters*, 46, 4007–4016. <https://doi.org/10.1029/2019GL082311>
- Herbert, R. J., Murray, B. J., Dobbie, S. J., & Koop, T. (2015). Sensitivity of liquid clouds to homogenous freezing parameterizations. *Geophysical Research Letters*, 42, 1599–1605. <https://doi.org/10.1002/2014GL062729>
- Hill, T. C. J., Moffett, B. F., Demott, P. J., Georgakopoulos, D. G., Stump, W. L., & Franc, G. D. (2014). Measurement of ice nucleation-active bacteria on plants and in precipitation by quantitative PCR. *Applied and Environmental Microbiology*, 80(4), 1256–1267. <https://doi.org/10.1128/AEM.02967-13>
- Hobbs, P. V., & Locatelli, J. D. (1969). Ice nuclei from a natural forest fire. *Journal of Applied Meteorology*, 8(5), 833.
- Hodshire, A. L., Akherati, A., Alvarado, M. J., Brown-Steiner, B., Jathar, S. H., Jimenez, J. L., et al. (2019). Aging effects on biomass burning aerosol mass and composition: A critical review of field and laboratory studies. *Environmental Science & Technology*, 53(17), 10,007–10,022. <https://doi.org/10.1021/acs.est.9b02588>
- Holden, M. A., Whale, T. F., Tarn, M. D., O'Sullivan, D., Walshaw, R. D., Murray, B. J., et al. (2019). High-speed imaging of ice nucleation in water proves the existence of active sites. *Science Advances*, 5(2), eaav4316. <https://doi.org/10.1126/sciadv.aav4316>
- Hoose, C., & Möhler, O. (2012). Heterogeneous ice nucleation on atmospheric aerosols: A review of results from laboratory experiments. *Atmospheric Chemistry and Physics*, 12(20), 9817–9854. <https://doi.org/10.5194/acp-12-9817-2012>

- Jiang, Q., Sun, Y. L., Wang, Z., & Yin, Y. (2015). Aerosol composition and sources during the Chinese Spring Festival: Fireworks, secondary aerosol, and holiday effects. *Atmospheric Chemistry and Physics*, 15(11), 6023–6034. <https://doi.org/10.5194/acp-15-6023-2015>
- Kamphus, M., Bittner-Mahl, M., Klimach, T., Drewnick, F., Keller, L., Cziczko, D. J., et al. (2010). Chemical composition of ambient aerosol, ice residues and cloud droplet residues in mixed-phase clouds: Single particle analysis during the Cloud and Aerosol Characterization Experiment (CLACE 6). *Atmospheric Chemistry and Physics*, 10(16), 8077–8095. <https://doi.org/10.5194/acp-10-8077-2010>
- Kanji, Z. A., Ladino, L. A., Wex, H., Boose, Y., Burkert-Kohn, M., Cziczko, D. J., & Krämer, M. (2017). Overview of ice nucleating particles. *Meteorological Monographs*, 58, 1.1–1.33. <https://doi.org/10.1175/AMSMONOGRAPHS-D-16-0006.1>
- Kanji, Z. A., Welti, A., Corbin, J. C., & Mensah, A. A. (2020). Black carbon particles do not matter for immersion mode ice nucleation. *Geophysical Research Letters*, 47, e2019GL086764. <https://doi.org/10.1029/2019GL086764>
- Kireeva, E. D., Popovicheva, O. B., Persiantseva, N. M., Khokhlova, T. D., & Shonija, N. K. (2009). Effect of black carbon particles on the efficiency of water droplet freezing. *Colloid Journal*, 71(3), 353–359. <https://doi.org/10.1134/S1061933X09030090>
- Koch, D., Schulz, M., Kinne, S., McNaughton, C., Spackman, J. R., Balkanski, Y., et al. (2009). Evaluation of black carbon estimations in global aerosol models. *Atmospheric Chemistry and Physics*, 9(22), 9001–9026. Retrieved from www.atmos-chem-phys.net/9/9001/2009/, <https://doi.org/10.5194/acp-9-9001-2009>
- Kumai, M. (1961). Snow crystals and the identification of the nuclei in the northern United States of America. *Journal of Meteorology*, 18(2), 139–150. [https://doi.org/10.1175/1520-0469\(1961\)018<0139:SCATIO>2.0.CO;2](https://doi.org/10.1175/1520-0469(1961)018<0139:SCATIO>2.0.CO;2)
- Lavanchy, V. M. H., Gäggeler, H. W., Schotterer, U., Schwikowski, M., & Baltensperger, U. (1999). Historical record of carbonaceous particle concentrations from a European high-alpine glacier (Colle Gnifetti, Switzerland). *Journal of Geophysical Research*, 104(D17), 21,227–21,236. <https://doi.org/10.1029/1999JD900408>
- Levin, E. J. T., McMeeking, G. R., DeMott, P. J., McCluskey, C. S., Carrico, C. M., Nakao, S., et al. (2016). Ice-nucleating particle emissions from biomass combustion and the potential importance of soot aerosol. *Journal of Geophysical Research: Atmospheres*, 121, 5888–5903. <https://doi.org/10.1002/2016JD024879>
- Li, J., Xu, T., Lu, X., Chen, H., Nizkorodov, S. A., Chen, J., et al. (2017). Online single particle measurement of fireworks pollution during Chinese New Year in Nanning. *Journal of Environmental Sciences*, 53, 184–195. <https://doi.org/10.1016/j.jes.2016.04.021>
- Lighty, J. A. S., Veranth, J. M., & Sarofim, A. F. (2000). Combustion aerosols: Factors governing their size and composition and implications to human health. *Journal of the Air and Waste Management Association*, 50(9), 1565–1618. <https://doi.org/10.1080/10473289.2000.10464197>
- Lin, C.-C. (2016). Journal of the Air & Waste Management Association A review of the impact of fireworks on particulate matter in ambient air. *Journal of the Air & Waste Management Association*, 66, 1171–1182. <https://doi.org/10.1080/10962247.2016.1219280>
- Lindsley, W. G. (2014). NIOSH Manual of Analytical Methods (NMAM), 5th Edition Filter pore size and aerosol sample collection. Retrieved from <https://www.cdc.gov/niosh/docs/2014-151/pdfs/chapters/chapter-fp.pdf>
- Liu, D. Y., Rutherford, D., Kinsey, M., & Prather, K. A. (1997). Real-time monitoring of pyrotechnically derived aerosol particles in the troposphere. *Analytical Chemistry*, 69(10), 1808–1814. <https://doi.org/10.1021/AC9612988>
- Lohmann, U., Diehl, K., Lohmann, U., & Diehl, K. (2006). Sensitivity studies of the importance of dust ice nuclei for the indirect aerosol effect on stratiform mixed-phase clouds. *Journal of the Atmospheric Sciences*, 63(3), 968–982. <https://doi.org/10.1175/JAS3662.1>
- Mahrt, F., Marcolli, C., David, R. O., Grönquist, P., Meier, E. J. B., Lohmann, U., & Kanji, Z. A. (2018). Ice nucleation abilities of soot particles determined with the Horizontal Ice Nucleation Chamber. *Atmospheric Chemistry and Physics*, 18, 13,363–13,392. <https://doi.org/10.5194/acp-18-13363-2018>
- McCluskey, C. S., DeMott, P. J., Prenni, A. J., Levin, E. J. T., McMeeking, G. R., Sullivan, A. P., et al. (2014). Characteristics of atmospheric ice nucleating particles associated with biomass burning in the US: Prescribed burns and wildfires. *Journal of Geophysical Research: Atmospheres*, 119, 10,458–10,470. <https://doi.org/10.1002/2014JD021980>
- McCluskey, C. S., Ovadnevaite, J., Rinaldi, M., Atkinson, J., Belosi, F., Ceburnis, D., et al. (2018). Marine and terrestrial organic ice-nucleating particles in pristine marine to continentally influenced Northeast Atlantic air masses. *Journal of Geophysical Research: Atmospheres*, 123, 6196–6212. <https://doi.org/10.1029/2017JD028033>
- Möhler, O., Benz, S., Saathoff, H., Schnaiter, M., Wagner, R., Schneider, J., et al. (2008). The effect of organic coating on the heterogeneous ice nucleation efficiency of mineral dust aerosols. *Environmental Research Letters*, 3(2), 025007. <https://doi.org/10.1088/1748-9326/3/2/025007>
- Moreno, T., Querol, X., Alastuey, A., Cruz Minguillón, M., Pey, J., Rodriguez, S., et al. (2007). Recreational atmospheric pollution episodes: Inhalable metalliferous particles from firework displays. *Atmospheric Environment*, 41(5), 913–922. <https://doi.org/10.1016/j.atmosenv.2006.09.019>
- Murray, B. J., O'Sullivan, D., Atkinson, J. D., & Webb, M. E. (2012). Ice nucleation by particles immersed in supercooled cloud droplets. *Chemical Society Reviews*, 41(19), 6519–6554. <https://doi.org/10.1039/c2cs35200a>
- O'Sullivan, D., Murray, B. J., Malkin, T. L., Whale, T. F., Umo, N. S., Atkinson, J. D., et al. (2014). Ice nucleation by fertile soil dusts: Relative importance of mineral and biogenic components. *Atmospheric Chemistry and Physics*, 14(4), 1853–1867. <https://doi.org/10.5194/acp-14-1853-2014>
- O'Sullivan, D. O., Adams, M. P., Tarn, M. D., Harrison, A. D., Vergara-Temprado, J., Porter, G. C., et al. (2018). Contributions of biogenic material to the atmospheric ice-nucleating particle population in North Western Europe. *Scientific Reports*, 8(1), 13821. <https://doi.org/10.1038/s41598-018-31981-7>
- Petters, M. D., & Wright, T. P. (2015). Revisiting ice nucleation from precipitation samples. *Geophysical Research Letters*, 42, 8758–8766. <https://doi.org/10.1002/2015GL065733>
- Petters, M. D., Parsons, M. T., Prenni, A. J., DeMott, P. J., Kreidenweis, S. M., Carrico, C. M., et al. (2009). Ice nuclei emissions from biomass burning. *Journal of Geophysical Research*, 114, D07209. <https://doi.org/10.1029/2008JD011532>
- Petzold, A., Ogren, J. A., Fiebig, M., Laj, P., Li, S. M., Baltensperger, U., et al. (2013). Geoscientific instrumentation methods and data systems recommendations for reporting “black carbon” measurements. *Atmospheric Chemistry and Physics*, 13(16), 8365–8379. <https://doi.org/10.5194/acp-13-8365-2013>
- Phillips, V. T. J., DeMott, P. J., Andronache, C., Phillips, V. T. J., DeMott, P. J., & Andronache, C. (2008). An empirical parameterization of heterogeneous ice nucleation for multiple chemical species of aerosol. *Journal of the Atmospheric Sciences*, 65(9), 2757–2783. <https://doi.org/10.1029/2007JD009201>

- material to the atmospheric ice-nucleating particle population in North Western Europe. *Scientific Reports*, 8(1), 13821. <https://doi.org/10.1038/s41598-018-31981-7>
- Petters, M. D., & Wright, T. P. (2015). Revisiting ice nucleation from precipitation samples. *Geophysical Research Letters*, 42, 8758–8766. <https://doi.org/10.1002/2015GL065733>
- Petters, M. D., Parsons, M. T., Prenni, A. J., DeMott, P. J., Kreidenweis, S. M., Carrico, C. M., et al. (2009). Ice nuclei emissions from biomass burning. *Journal of Geophysical Research*, 114, D07209. <https://doi.org/10.1029/2008JD011532>
- Petzold, A., Ogren, J. A., Fiebig, M., Laj, P., Li, S. M., Baltensperger, U., et al. (2013). Geoscientific instrumentation methods and data systems recommendations for reporting “black carbon” measurements. *Atmospheric Chemistry and Physics*, 13(16), 8365–8379. <https://doi.org/10.5194/acp-13-8365-2013>
- Phillips, V. T. J., DeMott, P. J., Andronache, C., Phillips, V. T. J., DeMott, P. J., & Andronache, C. (2008). An empirical parameterization of heterogeneous ice nucleation for multiple chemical species of aerosol. *Journal of the Atmospheric Sciences*, 65(9), 2757–2783. <https://doi.org/10.1175/2007JAS2546.1>
- Phillips, V. T. J., Demott, P. J., Andronache, C., Pratt, K. A., Prather, K. A., Subramanian, R., & Twohy, C. (2013). Improvements to an empirical parameterization of heterogeneous ice nucleation and its comparison with observations. *Journal of the Atmospheric Sciences*, 70(2), 378–409. <https://doi.org/10.1175/JAS-D-12-080.1>

- Pope, R. J., Marshall, A. M., & O'Kane, B. O. (2016). Observing UK Bonfire Night pollution from space: Analysis of atmospheric aerosol. *Weather*, 71(11), 288–291. <https://doi.org/10.1002/wea.2914>
- Popovicheva, O., Kireeva, E., Persiantseva, N., Khokhlova, T., Shonija, N., Tishkova, V., & Demirdjian, B. (2008). Effect of soot on immersion freezing of water and possible atmospheric implications. *Atmospheric Research*, 90(2–4), 326–337. <https://doi.org/10.1016/j.atmosres.2008.08.004>
- Pósfai, M., Gelencsér, A., Simonics, R., Arató, K., Li, J., Hobbs, P. V., & Buseck, P. R. (2004). Atmospheric tar balls: Particles from biomass and biofuel burning. *Journal of Geophysical Research*, 109, D06213. <https://doi.org/10.1029/2003jd004169>
- Pratt, K. A., DeMott, P. J., French, J. R., Wang, Z., Westphal, D. L., Heymsfield, A. J., et al. (2009). In situ detection of biological particles in cloud ice-crystals. *Nature Geoscience*, 2(6), 398–401. <https://doi.org/10.1038/NNGEO521>
- Prenni, A. J., Demott, P. J., Sullivan, A. P., Sullivan, R. C., Kreidenweis, S. M., & Rogers, D. C. (2012). Biomass burning as a potential source for atmospheric ice nuclei: Western wildfires and prescribed burns. *Geophysical Research Letters*, 39, L11805. <https://doi.org/10.1029/2012GL051915>
- Prenni, A. J., Petters, M. D., Kreidenweis, S. M., Heald, C. L., Martin, S. T., Artaxo, P., et al. (2009). Relative roles of biogenic emissions and Saharan dust as ice nuclei in the Amazon basin. *Nature Geoscience*, 2(6), 402–405. <https://doi.org/10.1038/ngeo517>
- Reyes-Villegas, E., Priestley, M., Ting, Y. C., Haslett, S., Bannan, T., le Breton, M., et al. (2018). Simultaneous aerosol mass spectrometry and chemical ionisation mass spectrometry measurements during a biomass burning event in the UK: Insights into nitrate chemistry. *Atmos. Chemical Physics*, 18(6), 4093–4111. <https://doi.org/10.5194/acp-18-4093-2018>
- Rosenfeld, D., Yu, X., Liu, G., Xu, X., Zhu, Y., Yue, Z., et al. (2011). Glaciation temperatures of convective clouds ingesting desert dust, air pollution and smoke from forest fires. *Geophysical Research Letters*, 38, L21804. <https://doi.org/10.1029/2011GL049423>
- Sanchez-Marroquin, A., Hedges, D. H., Hiscock, M., Parker, S. T., Rosenberg, P. D., Trembath, J., et al. (2019). Characterisation of the filter inlet system on the BAE-146 research aircraft and its use for size resolved aerosol composition measurements. *Atmospheric Measurement Techniques Discussions*, 1–35. <https://doi.org/10.5194/amt-2019-196>
- Šantl-Temkiv, T., Sahyoun, M., Finster, K., Hartmann, S., Augustin-Bauditz, S., Stratmann, F., et al. (2015). Characterization of airborne ice-nucleation-active bacteria and bacterial fragments. *Atmospheric Environment*, 109, 105–117. <https://doi.org/10.1016/j.atmosenv.2015.02.060>
- Schill, G. P., Jathar, S. H., Kodros, J. K., Levin, E. J. T., Galang, A. M., Friedman, B., et al. (2016). Ice-nucleating particle emissions from photochemically aged diesel and biodiesel exhaust. *Geophysical Research Letters*, 43, 5524–5531. <https://doi.org/10.1002/2016GL069529>
- Schlosser, J. S., Braun, R. A., Bradley, T., Dadashazar, H., MacDonald, A. B., Aldhaif, A. A., et al. (2017). Analysis of aerosol composition data for western United States wildfires between 2005 and 2015: Dust emissions, chloride depletion, and most enhanced aerosol constituents. *Journal of Geophysical Research: Atmospheres*, 122, 8951–8966. <https://doi.org/10.1002/2017JD026547>
- Schnell, R. C., Pueschel, R. F., Weickmann, H. K., & Wellman, D. L. (1980). Ice nucleus and aerosol measurements in the plume of the Johnstown, PA, steel mill. *Geophysical Research Letters*, 7(5), 397–400. <https://doi.org/10.1029/GL007i005p00397>
- Singh, A., Bloss, W. J., & Pope, F. D. (2015). Remember, remember the 5th of November; gunpowder, particles and smog. *Weather*, 70(11), 320–324. <https://doi.org/10.1002/wea.2587>
- Soo, J.-C., Monaghan, K., Lee, T., Kashon, M., & Harper, M. (2016). Air sampling filtration media: Collection efficiency for respirable size-selective sampling. *Aerosol Science and Technology: The Journal of the American Association for Aerosol Research*, 50(1), 76–87. Retrieved from <http://www.ncbi.nlm.nih.gov/pubmed/26834310>
- Spracklen, D. V., Carslaw, K. S., Pöschl, U., Rap, A., & Forster, P. M. (2011). Global cloud condensation nuclei influenced by carbonaceous combustion aerosol. *Atmospheric Chemistry and Physics*, 11(17), 9067–9087. <https://doi.org/10.5194/acp-11-9067-2011>
- Stein, A. F., Draxler, R. R., Rolph, G. D., Stunder, B. J. B., Cohen, M. D., & Ngan, F. (2015). NOAA's hysplit atmospheric transport and dispersion modeling system. *Bulletin of the American Meteorological Society*, 96(12), 2059–2077. <https://doi.org/10.1175/BAMS-D-14-00110.1>
- Storelmo, T. (2017). Aerosol effects on climate via mixed-phase and ice clouds. *Annual Review of Earth and Planetary Sciences*, 45(1), 199–222. <https://doi.org/10.1146/annurev-earth-060115-012240>
- Tan, I., Storelmo, T., & Zelinka, M. D. (2016). Observational constraints on mixed-phase clouds imply higher climate sensitivity. *Science (New York, N.Y.)*, 352(6282), 224–227. <https://doi.org/10.1126/science.aad5300>
- Tarn, M. D., Sikora, S. N. F., Porter, G. C. E., O'Sullivan, D., Adams, M., Whale, T. F., et al. (2018). The study of atmospheric ice-nucleating particles via microfluidically generated droplets. *Microfluidics and Nanofluidics*, 22(5), 52–25. <https://doi.org/10.1007/s10404-018-2069-x>
- Twohy, C. H., DeMott, P. J., Pratt, K. A., Subramanian, R., Kok, G. L., Murphy, S. M., et al. (2010). Relationships of biomass-burning aerosols to ice in orographic wave clouds. *Journal of the Atmospheric Sciences*, 67(8), 2437–2450. <https://doi.org/10.1175/2010JAS3310.1>
- Ullrich, R., Hoose, C., Möhler, O., Niemand, M., Wagner, R., Höhler, K., et al. (2017). A new ice nucleation active site parameterization for desert dust and soot. *Journal of the Atmospheric Sciences*, 74(3), 699–717. <https://doi.org/10.1175/JAS-D-16-0074.1>
- Umo, N. S., Murray, B. J., Baeza-Romero, M. T., Jones, J. M., Lea-Langton, A. R., Malkin, T. L., et al. (2015). Ice nucleation by combustion ash particles at conditions relevant to mixed-phase clouds. *Atmospheric Chemistry and Physics*, 15(9), 5195–5210. <https://doi.org/10.5194/acp-15-5195-2015>
- Umo, N. S., Wagner, R., Ullrich, R., Kiselev, A., Saathoff, H., Weidler, P. G., et al. (2019). Enhanced ice nucleation activity of coal fly ash aerosol particles initiated by ice-filled pores. *Atmospheric Chemistry and Physics*, 19(13), 8783–8800. <https://doi.org/10.5194/acp-19-8783-2019>
- Vali, G., DeMott, P. J., Möhler, O., & Whale, T. F. (2015). Technical note: A proposal for ice nucleation terminology. *Atmospheric Chemistry and Physics*, 15(18). <https://doi.org/10.5194/acp-15-10263-2015>
- Vali, G. (1971). Quantitative evaluation of experimental results on the heterogeneous freezing nucleation of supercooled liquids. *Journal of the Atmospheric Sciences*, 28(3), 402–409. <https://doi.org/10.1175/1520-0469>
- Vergara-Temprado, J., Holden, M. A., Orton, T. R., O'Sullivan, D., Umo, N. S., Browne, J., et al. (2018). Is black carbon an unimportant ice-nucleating particle in mixed-phase clouds? *Journal of Geophysical Research: Atmospheres*, 123, 4273–4283. <https://doi.org/10.1002/2017JD027831>
- Westbrook, C. D., & Illingworth, A. J. (2011). Evidence that ice forms primarily in supercooled liquid clouds at temperatures > -27°C. *Geophysical Research Letters*, 38, L14808. <https://doi.org/10.1029/2011GL048021>
- Whale, T. F., Murray, B. J., O'Sullivan, D., Wilson, T. W., Umo, N. S., Baustian, K. J., et al. (2015). A technique for quantifying heterogeneous ice nucleation in microlitre supercooled water droplets. *Atmospheric Measurement Techniques*, 8(6), 2437–2447. <https://doi.org/10.5194/amt-8-2437-2015>
- Whale, T. F., Rosillo-Lopez, M., Murray, B. J., & Salzmann, C. G. (2015). Ice nucleation properties of oxidized carbon nanomaterials. *Journal of Physical Chemistry Letters*, 6(15), 3012–3016. <https://doi.org/10.1021/acs.jpcclett.5b01096>

- Wofsy, S. C. (2011). HIPPER Pole-to-Pole Observations (HIPPO): Fine-grained, global-scale measurements of climatically important atmospheric gases and aerosols. *Philosophical Transactions of the Royal Society A*, 369, 2073–2086. <https://doi.org/10.1098/rsta.2010.0313>
- Wright, T. P., Petters, M. D., Hader, J. D., Morton, T., & Holder, A. L. (2013). Minimal cooling rate dependence of ice nuclei activity in the immersion mode. *Journal of Geophysical Research: Atmospheres*, 118, 10,535–10,543. <https://doi.org/10.1002/jgrd.50810>
- Zhang, Y., Zhang, Q., Cheng, Y., Su, H., Kecorius, S., Wang, Z., et al. (2016). Measuring the morphology and density of internally mixed black carbon with SP2 and VTDMA: New insight into the absorption enhancement of black carbon in the atmosphere. *Atmospheric Measurement Techniques*, 9(4), 1833–1843. <https://doi.org/10.5194/amt-9-1833-2016>
- Zhao, B., Wang, Y., Gu, Y., Liou, K. N., Jiang, J. H., Fan, J., et al. (2019). Ice nucleation by aerosols from anthropogenic pollution. *Nature Geoscience*, 12(8), 602–607. <https://doi.org/10.1038/s41561-019-0389-4>

